The Double-Density Dual-Tree DWT

Ivan W. Selesnick, *Member, IEEE*

***Abstract*—This paper introduces the double-density dual-tree discrete wavelet transform (DWT), which is a DWT that combines the double-density DWT and the dual-tree DWT, each of which has its own characteristics and advantages. The transform corresponds to a new family of dyadic wavelet tight frames based on two scaling functions and four distinct wavelets. One pair of the four wavelets are designed to be offset from the other pair of wavelets so that the integer translates of one wavelet pair fall midway between the integer translates of the other pair. Simultaneously, one pair of wavelets are designed to be approximate Hilbert transforms of the other pair of wavelets so that two complex (approximately analytic) wavelets can be formed. Therefore, they can be used to implement complex and directional wavelet transforms. The paper develops a design procedure to obtain finite impulse response (FIR) filters that satisfy the numerous constraints imposed. This design procedure employs a fractional-delay allpass filter, spectral factorization, and filterbank completion. The solutions have vanishing moments, compact support, a high degree of smoothness, and are nearly shift-invariant.**

***Index Terms*—Dual-tree complex wavelet transform, frame.**

I. Introduction

In this paper, we introduce the *double-density dual-tree* DWT, which is an overcomplete discrete wavelet transform (DWT) designed to simultaneously possess the properties of the double-density DWT [24], [26] and the dual-tree complex DWT [11]–[13]. The double-density DWT and the dual-tree complex DWT are similar in several respects (they are both overcomplete by a factor of two, they are both nearly shift-invariant, and they are both based on FIR perfect reconstruction filter banks), but they are quite different from one another in other important respects. Both wavelet transforms can outperform the critically sampled DWT for several signal processing applications, but they do so for different reasons. It is therefore natural to investigate the possibility of a single wavelet transform that has the characteristics of both the double-density DWT and dual-tree complex DWT. This is the motivation for the development of the double-density dual-tree DWT described in this paper.

The development of the double-density DWT was motivated in part by the *undecimated* DWT. The undecimated DWT is exactly shift-invariant, and for denoising, it performs substantially better than the critically sampled DWT [5], [15]–[17]. The double-density DWT is based on a single scaling function and two distinct wavelets, where the two wavelets are designed to be offset from one another by one half—the integer translates of one wavelet fall midway between the integer translates of the other wavelet

$$\psi_2(t) \approx \psi_1(t - 0.5). \tag{1}$$

In this way, the double-density DWT approximates the continuous wavelet transform (having more wavelets than necessary gives a closer spacing between adjacent wavelets within the same scale). The design of wavelet frames (or *overcomplete* bases) of this type is described in [24]. Specifically, [24] describes the design of wavelet filters of minimal support with vanishing moment properties (analogous to Daubechies' orthonormal wavelet bases but now in the oversampled case). The resulting wavelets are very smooth with short support, and the transform is nearly shift invariant.

On the other hand, the development of the dual-tree DWT was motivated by the special properties of complex wavelet transforms. Numerous researchers in vision and image processing have suggested that an effective waveform for image processing is a Gabor atom (or Gabor patch). However, it is difficult to do this with the traditional two-dimensional (2-D) critically sampled discrete wavelet transform. However, Kingsbury has demonstrated that it is possible to develop a wavelet transform with Gabor-like complex-valued wavelets by employing two suitably designed critically sampled DWTs in parallel. It is required that the wavelets corresponding to each of the two DWTs form an approximate Hilbert transform pair

$$\psi_g(t) \approx \mathcal{H}\{\psi_h(t)\}. \tag{2}$$

The parallel combination of two DWTs designed to satisfy (2) is called the dual-tree complex DWT [12]. Kingsbury has demonstrated that the dual-tree complex DWT can lead to substantial improvements in wavelet-based signal processing.

The design of wavelets for the dual-tree DWTs described in relied on filter coefficient optimization to minimize aliasing in a multistage filter bank. The dual-tree DWT was further analyzed in [25], which introduces a theorem describing how the filter coefficients can be chosen to obtain two wavelet bases where the two wavelets form a Hilbert transform pair (or complex dual-tree). The characterization theorem helps explain the result by Kingsbury and also makes possible the design of new dual-tree wavelet bases with vanishing moments. The new examples presented in [25] were obtained using Gröbner bases to solve certain nonlinear design equations arising from the characterization theorem, but because it is desirable to have a more flexible design procedure (not based on Gröbner bases), this work was further developed, and a design algorithm based on spectral-factorization was described in [23] and [27]. This design algorithm extends the algorithm developed by Daubechies for the construction of orthogonal wavelet bases to the new problem arising from the dual-tree complex DWT.

Manuscript received July 17, 2001; revised May 28, 2003. This work was supported by the National Science Foundation under CAREER Grant CCR-9875452. The associate editor coordinating the review of this manuscript and approving it for publication was Prof. Arnab K. Shaw.

The author is with the Department of Electrical and Computer Engineering, Polytechnic University, Brooklyn, NY 11202 USA (e-mail: selesi@poly.edu).

Digital Object Identifier 10.1109/TSP.2004.826174

The differences between the double-density DWT and the dual-tree DWT can be clarified with the following comparisons.

1) In the dual-tree DWT, the two wavelets form an approximate Hilbert transform pair, whereas in the double-density DWT, the two wavelets are offset by one half.
2) For the dual-tree DWT, there are fewer degrees of freedom for design (achieving the Hilbert pair property adds constraints), whereas for the double-density DWT, there are more degrees of freedom for design.
3) Different filterbank structures are used to implement the dual-tree and double-density DWTs.
4) The dual-tree DWT can be interpreted as a complex-valued wavelet transform, which is useful for signal modeling and denoising (the double-density DWT cannot be interpreted as such).
5) The dual-tree DWT can be used to implement 2-D transforms with directional Gabor-like wavelets, which is highly desirable for image processing (the double-density DWT cannot be, although it can be used in conjunction with specialized post-filters to implement a complex wavelet transform with low-redundancy, as developed in [8]).

The double-density dual-tree DWT presented in this paper, which is designed to simultaneously possess the properties of the double-density DWT and the dual-tree DWT, is based on two distinct scaling functions and four distinct wavelets

$$\psi_{h,i}(t), \quad \psi_{g,i}(t), \quad i = 1, 2$$

where the two wavelets $\psi_{h,i}(t)$ are offset from one another by one half, as is $\psi_{g,i}(t)$:

$$\psi_{h,1}(t) \approx \psi_{h,2}(t - 0.5), \quad \psi_{g,1}(t) \approx \psi_{g,2}(t - 0.5) \tag{3}$$

and where the two wavelets $\psi_{g,1}(t)$ and $\psi_{h,1}(t)$ form an approximate Hilbert transform pair, as do $\psi_{g,2}(t)$ and $\psi_{h,2}(t)$:

$$\psi_{g,1}(t) \approx \mathcal{H}\{\psi_{h,1}(t)\}, \quad \psi_{g,2}(t) \approx \mathcal{H}\{\psi_{h,2}(t)\}. \tag{4}$$

The design procedure for the double-density dual-tree DWT introduced here draws on the design procedures for the double-density DWT and the dual-tree DWT described in [3], [23], [24], and [27]. This design procedure is based on the flat-delay filter, spectral factorization, and paraunitary filterbank completion. The solutions have vanishing moments and compact support. The resulting wavelets are much smoother than the dual-tree wavelets, and unlike the double-density wavelets, they form approximate Hilbert transform pairs. The design procedure also includes a parameter L, that determines the degree to which the approximation (4) is satisfied.

The intended applications of the double-density dual-tree DWT are the same as those of the dual-tree complex DWT (for example, image denoising, enhancement, and segmentation; and motion estimation and compensation). Because the wavelets of the double-density dual-tree DWT are more closely spaced than those of the dual-tree DWT, algorithms like matching pursuits have a greater number of atoms with which to approximate a given signal.

We also wish to note that although the structure of the DWT introduced in this paper is different, the goals are similar to those described in [29], which introduced *shiftable multiscale transforms*. In addition, the double-density DWT is an example of an *affine* frame; see [3], [4], [7], [18], [19], [21], and [22]. The value of Hilbert pairs of wavelet bases has also been discussed in [1], [2], [9], [28], [29].

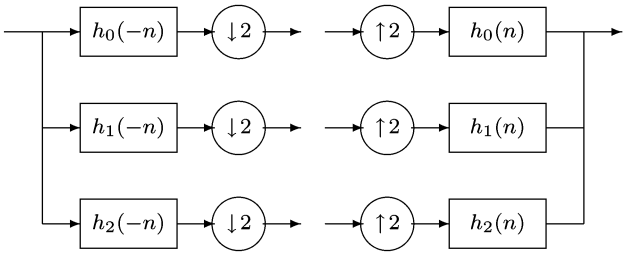

Fig. 1. Oversampled analysis and synthesis filterbank.

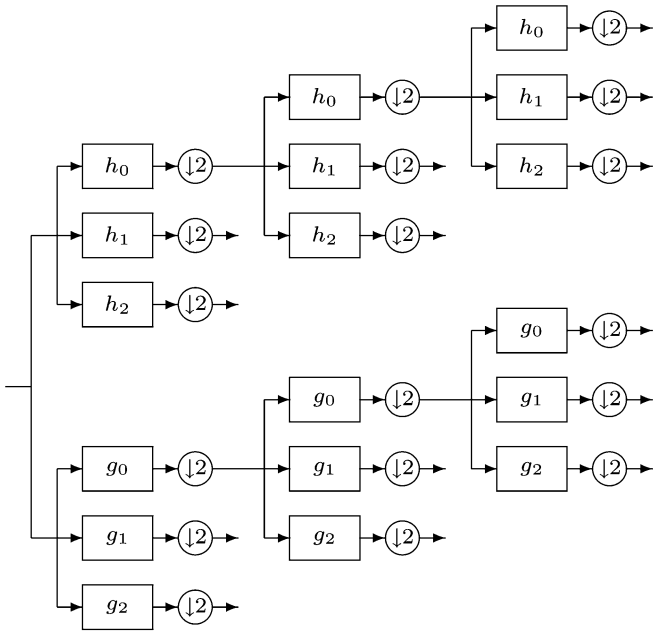

Fig. 2. Iterated filterbank for the double-density dual-tree DWT.

II. Preliminaries

The dual-tree DWT is based on concatenating two critically sampled DWTs. The filterbank structure corresponding to the dual-tree DWT simply consists of two critically sampled iterated filterbanks operating in parallel. The performance gains provided by the dual-tree DWT come from designing the filters in the two filterbanks appropriately.

The double-density dual-tree DWT proposed in this paper is based on concatenating two oversampled DWTs. The filterbank structure corresponding to the double-density dual-tree DWT consists of two oversampled iterated filterbanks operating in parallel, similar to the dual-tree DWT. The oversampled filter bank is illustrated in Fig. 1. The iterated oversampled filter bank, corresponding to the implementation of the double-density dual-tree, is illustrated in Fig. 2. We will denote the filters in the first filterbank by $h_i(n)$ and the filters in the second filterbank by $g_i(n)$, for $i = 0, 1, 2$. Note that in each of the filterbanks to be considered in this paper, the synthesis filters

are the time-reversed versions of the analysis filters. The goal will be to design the six FIR filters so that they do the following.

i) They satisfy the perfect reconstruction property.
ii) The wavelets form two (approximate) Hilbert transform pairs.
iii) The wavelets have specified vanishing moments.
iv) The filters are of short support.

The Z-transform of $h_i(n)$ is denoted by $H_i(z)$

$$H_i(z) = \mathrm{ZT}\{h_i(n)\} := \sum_n h_i(n) z^{-n}$$

and $G_i(z)$ is similarly defined. Throughout the paper, it is assumed that all filter coefficients $h_i(n), g_i(n)$ are real valued. The frequency response $H_i(e^{j\omega})$ is given by

$$H_i(e^{j\omega}) = \mathrm{DTFT}\{h_i(n)\} := \sum_n h_i(n) e^{-jn\omega}$$

and $G_i(e^{j\omega})$ is similarly defined. The filters $h_i(n)$ and $g_i(n)$ should satisfy the perfect reconstruction (PR) conditions. From basic multirate identities, the PR conditions are the following:

$$\sum_{i=0}^{2} H_i(z) H_i(1/z) = 2 \tag{5}$$

$$\sum_{i=0}^{2} H_i(z) H_i(-1/z) = 0 \tag{6}$$

and

$$\sum_{i=0}^{2} G_i(z) G_i(1/z) = 2 \tag{7}$$

$$\sum_{i=0}^{2} G_i(z) G_i(-1/z) = 0. \tag{8}$$

The scaling and wavelet functions are defined implicitly through the dilation and wavelet equations

$$\phi_h(t) = \sqrt{2} \sum_n h_0(n) \phi_h(2t-n)$$
$$\psi_{h,1}(t) = \sqrt{2} \sum_n h_1(n) \phi_h(2t-n)$$
$$\psi_{h,2}(t) = \sqrt{2} \sum_n h_2(n) \phi_h(2t-n)$$

where $\phi_g(t)$ and $\psi_{g,i}(t)$ are defined similarly. The Fourier transforms of the scaling functions and wavelets will be denoted as

$$\Phi_h(\omega) = \mathcal{F}\{\phi_h(t)\}, \quad \Phi_g(\omega) = \mathcal{F}\{\phi_g(t)\}$$
$$\Psi_{h,i}(\omega) = \mathcal{F}\{\psi_{h,i}(t)\}, \quad \Psi_{g,i}(\omega) = \mathcal{F}\{\psi_{g,i}(t)\}.$$

The Hilbert transform of a function $f(t)$ will be denoted as $\mathcal{H}\{f(t)\}$. Following the work by Kingsbury, we want the wavelets to form Hilbert transform pairs

$$\psi_{g,1}(t) = \mathcal{H}\{\psi_{h,1}(t)\} \tag{9}$$
$$\psi_{g,2}(t) = \mathcal{H}\{\psi_{h,2}(t)\}. \tag{10}$$

Recalling the definition of the Hilbert transform, this means that

$$\Psi_{g,i}(\omega) = \begin{cases} -j\Psi_{h,i}(\omega), & \omega > 0 \\ j\Psi_{h,i}(\omega), & \omega < 0. \end{cases} \tag{11}$$

III. Filter Constraints for Hilbert Pair Property

Because the DWT is implemented using discrete-time filterbanks and because the discrete-time filters $h_i(n)$ and $g_i(n)$ define the wavelets, it is necessary to translate the Hilbert transform relations (9) and (10) into constraints to be imposed on the filterbank, that is, what constraints should the filters $h_i(n)$ and $g_i(n)$ satisfy so that $\psi_{h,i}(t)$ and $\psi_{g,i}(t)$ form a Hilbert pair? That is the question addressed in this section.

If $\psi_{h,i}(t)$ and $\psi_{g,i}(t)$ form a Hilbert transform pair, then $|\Psi_{h,i}(\omega)| = |\Psi_{g,i}(\omega)|$. This suggests, from the infinite product formula, that we should have $|G_i(e^{j\omega})| = |H_i(e^{j\omega})|$, for $i = 0, 1, 2$. That is, the filters should be related as

$$G_i(e^{j\omega}) = H_i(e^{j\omega})\, e^{-j\theta_i(\omega)} \tag{12}$$

where $\theta_i(\omega)$ are 2π-periodic. However, how should the three phase functions $\theta_i(\omega)$ be selected to have $\psi_{g,i}(t) = \mathcal{H}\{\psi_{h,i}(t)\}$?

The characterization of Hilbert pairs of wavelet bases in [25] involved a similar problem; however, in that problem, the highpass filter $H_1(z)$ is fully determined by the lowpass filter $H_0(z)$ and there was no filter $H_2(z)$. In the oversampled filterbank considered here, the highpass filters $H_1(z)$ and $H_2(z)$ are not fully determined by the lowpass filter $H_0(z)$; however, the approach introduced in [25] carries over as follows.

From the infinite product formula, we can derive as in [25] the following expression relating $\Phi_g(\omega)$ and $\Phi_h(\omega)$:

$$\Phi_g(\omega) = \Phi_h(\omega) \exp\left(-j \sum_{k=1}^{\infty} \theta_0(\omega/2^k) \right).$$

Similarly, we can derive the following expression relating $\Psi_{g,i}(\omega)$ and $\Psi_{h,i}(\omega)$:

$$\Psi_{g,i}(\omega) = \Psi_{h,i}(\omega) \times \exp\left(-j \left[\theta_i(\omega/2) + \sum_{k=2}^{\infty} \theta_0(\omega/2^k) \right] \right) \tag{13}$$

for $i = 1, 2$. From (11) and (13), we see that $\theta_i(\omega)$ must satisfy the following condition:

$$\theta_i(\omega/2) + \sum_{k=2}^{\infty} \theta_0(\omega/2^k) = \begin{cases} 0.5\pi, & \omega > 0 \\ -0.5\pi, & \omega < 0 \end{cases}, \quad i = 1, 2. \tag{14}$$

Following the derivation in [25] for orthogonal wavelet bases, we find that for the wavelet frames considered here, if the 2π-periodic functions $\theta_i(\omega)$ are defined as

$$\theta_0(\omega) = \frac{\omega}{2}, \quad |\omega| < \pi \tag{15}$$

and

$$\theta_i(\omega) = -\theta_0(\omega - \pi), \quad i = 1, 2 \tag{16}$$

then (14) holds, and therefore, $\{\psi_{h,i}(t), \psi_{g,i}(t)\}$ form a Hilbert transform pair for $i = 1, 2$.

IV. Filter Design for the Double-Density Dual-Tree DWT

The design problem can be stated as follows. Given $K_i, i = 0, 1, 2$, find six FIR filters $h_i(n), g_i(n)$ of short support satisfying

1) the perfect reconstruction conditions (5)–(8);
2) the Hilbert pair relations (4) or, equivalently, (15) and (16), which should be nearly satisfied;
3) zero moment conditions
$$\int t^k \psi_{h,i}(t)\, dt = \int t^k \psi_{g,i}(t)\, dt = 0, \quad i = 1, 2$$
for $0 \le k \le K_i - 1$, where K_1, K_2 are specified;
4) lowpass zeros at $\omega = \pi$, where the factor $(1 + z^{-1})^{K_0}$ should divide both $H_0(z)$ and $G_0(z)$;
5) the shift property (3).

As discussed in [24], by making $K_0 > K_1, K_0 > K_2$, we can obtain wavelets with a high degree of smoothness that also have the shift property (3). As in [24], it is unnecessary to specify any explicit constraint to ensure that $\psi_{h,1}(t) \approx \psi_{h,2}(t - 0.5)$; it is sufficient that K_0 exceeds K_1 and K_2. Then, by completing the filterbank as described below and in [24], it is possible to obtain two wavelets where one wavelet is similar to the other translated by one half. We do not have a proof that the shift property can always be obtained using the design procedure below; however, in our examples, we have found that the algorithm we describe does produce sets of wavelets that do satisfy (3).

The design procedure for the double-density dual-tree DWT introduced here draws on the design procedures for the double-density DWT and the dual-tree DWT described in [3], [23], [24], and [27]. We propose, for the double-density dual-tree DWT, that the set of filters take the following form:

$$H_0(z) = D(z)(1 + z^{-1})^{K_0} Q_0(z) \tag{17}$$
$$H_1(z) = (-z)^{-L} D(-1/z)(1 - z^{-1})^{K_1} Q_1(z) \tag{18}$$
$$H_2(z) = (-z)^{-L} D(-1/z)(1 - z^{-1})^{K_2} Q_2(z) \tag{19}$$
$$G_0(z) = z^{-L} D(1/z)(1 + z^{-1})^{K_0} Q_0(z) \tag{20}$$
$$G_1(z) = D(-z)(1 - z^{-1})^{K_1} Q_1(z) \tag{21}$$
$$G_2(z) = D(-z)(1 - z^{-1})^{K_2} Q_2(z). \tag{22}$$

Equivalently

$$h_0(n) = d(n) * s_0(n) * q_0(n) \tag{23}$$
$$h_1(n) = (-1)^n d(L - n) * s_1(n) * q_1(n) \tag{24}$$
$$h_2(n) = (-1)^n d(L - n) * s_2(n) * q_2(n) \tag{25}$$
$$g_0(n) = d(L - n) * s_0(n) * q_0(n) \tag{26}$$
$$g_1(n) = (-1)^n d(n) * s_1(n) * q_1(n) \tag{27}$$
$$g_2(n) = (-1)^n d(n) * s_2(n) * q_2(n) \tag{28}$$

where

$$s_0(n) = \binom{K_0}{n} = \frac{K_0!}{(K_0 - n)!n!}$$
$$s_i(n) = (-1)^n \binom{K_i}{n}, \quad i = 1, 2.$$

These expressions incorporate the moment properties. There are four transfer functions $D(z)$ and $Q_i(z), i = 0, 1, 2$, which will be determined according to the remaining properties (PR conditions and approximate Hilbert pair conditions). It will be illustrated, in the examples below, that a wavelet frame with the sought properties can be obtained with a set of filters taking the above form. $D(z)$ will be determined first. $D(z)$ will be determined so that the Hilbert pair relations are approximately satisfied. $Q_0(z)$ will be determined second; then, the two lowpass filters $H_0(z)$ and $G_0(z)$ will be known. $Q_1(z)$ and $Q_2(z)$ will then be obtained by filterbank completion (paraunitary extension), as described in Section V.

From (17) and (20), we can write

$$G_0(z) = H_0(z) \frac{z^{-L} D(1/z)}{D(z)} \tag{29}$$

where we can recognize that the transfer function

$$A(z) := \frac{z^{-L} D(1/z)}{D(z)} \tag{30}$$

is an allpass system, $|A(e^{j\omega})| = 1$, or $A(e^{j\omega}) = e^{-j\theta_a(\omega)}$ for some 2π-periodic phase function $\theta_a(\omega)$. Then, from (29), we have $G_0(e^{j\omega}) = H_0(e^{j\omega})\, e^{-j\theta_a(\omega)}$; therefore, referring to (12), we have $\theta_0(\omega) = \theta_a(\omega)$. The phase difference $\theta_0(\omega)$ is given by the phase function of the allpass filter $A(z)$. Similarly, from (18)–(19) and (21)–(22), we can write

$$G_i(z) = A(-1/z) H_i(z), \quad i = 1, 2$$

where the transfer function $A(-1/z)$ is also allpass. We have, for $i = 1, 2$

$$\begin{aligned} G_i(e^{j\omega}) &= \overline{A(-e^{-j\omega})}\, H_i(e^{j\omega}) \\ &= \overline{A(e^{j(\omega-\pi)})}\, H_i(e^{j\omega}) \\ &= e^{j\theta_a(\omega-\pi)}\, H_i(e^{j\omega}). \end{aligned}$$

That is, $\theta_i(\omega) = -\theta_a(\omega - \pi)$ for $i = 1, 2$.

Therefore, with filters having the forms proposed in (17)–(22), the phase difference $\theta_0(\omega)$ is identical to the phase function $\theta_a(\omega)$ of the allpass system $A(z)$, whereas for $i = 1, 2$, the phase difference $\theta_i(\omega)$ is given by $-\theta_a(\omega - \pi)$. From (15) and (16), it follows directly that $D(z)$ should be chosen so that the phase function $\theta_a(\omega)$ of the all-pass system is $\omega/2$ for $|\omega| < \pi$. Because the phase function of $A(z)$ cannot equal $\omega/2$ exactly when $D(z)$ is of finite degree, it is necessary to employ an approximation. An allpass system whose phase function approximates $\tau\omega$ for some range of ω is simply a fractional-delay allpass filter (see [14] for a review of such systems). This type of system delays its input signal by τ samples.

We will take $A(z)$ to be a maximally flat fractional-delay allpass filter. (Any fractional-delay allpass filter could be used here.) The maximally flat type, which is accurate with a degree (L) of tangency at $\omega = 0$, is given by the following formula, adapted from [30]:

$$D(z) = 1 + \sum_{n=1}^{L} d(n) z^{-n}$$

where

$$d(n) = (-1)^n \binom{L}{n} \frac{(\tau - L)_n}{(\tau + 1)_n} \tag{31}$$

and where $(x)_n$ represents the rising factorial

$$(x)_n := \underbrace{(x)(x+1)\cdots(x+n-1)}_{n \text{ terms}}.$$

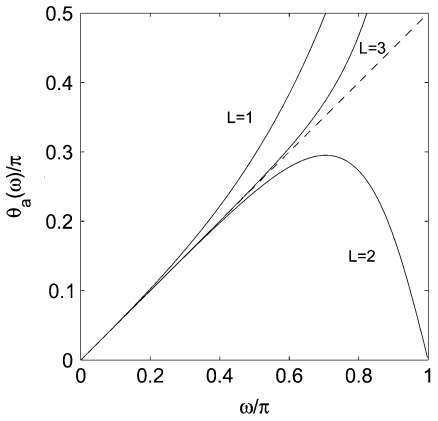

Fig. 3. Phase function $\theta_a(\omega)$ of the maximally flat fractional-delay allpass filter with $\tau = 0.5$ and $L = 1, 2, 3$.

With this $D(z)$, we have the approximation $A(z) \approx z^{-\tau}$ around $z = 1$ or, equivalently, $A(e^{j\omega}) \approx e^{-j\tau\omega}$ around $\omega = 0$; therefore, we have $\theta_a(\omega) \approx \tau\omega$ around $\omega = 0$.

The coefficients $d(n)$ in (31) can be computed very efficiently with the following recursion:

$$\begin{aligned} d(0) &= 1 \\ d(n+1) &= d(n) \cdot \frac{(L-n)(L-n-\tau)}{(n+1)(n+1+\tau)} \\ 0 &\le n \le L-1. \end{aligned}$$

In our problem, we will use $d(n)$ in (31) with $\tau = 1/2$. For example, with $L = 1$, we have $d(n) = \{1, 1/3\}$, for $n = 0, 1$. With $L = 2$, we have $d(n) = \{1, 2, 1/5\}$, for $n = 0, 1, 2$. With $L = 3$, we have $d(n) = \{1, 5, 3, 1/7\}$, for $n = 0, 1, 2, 3$. The phase function $\theta_a(\omega)$ of the maximally flat fractional-delay allpass filter $A(z)$ in (30) with these $D(z)$ are shown in Fig. 3. For larger values of L, an improved approximation to $\omega/2$ is obtained. The line $\omega/2$ is indicated in the figure by the dashed line. Note that the behavior of $\theta_a(\omega)$ is not important in the stop band of the lowpass filter $H_0(z)$; therefore, the deviation of $\theta_a(\omega)$ from $\omega/2$ near $\omega = \pi$ is not relevant.

With $D(z)$ chosen as described here, the filters (17)–(22) automatically satisfy (approximately) the Hilbert pair property and have the specified number of vanishing moments. The remaining design problem is to find $Q_i(z)$ (of minimal degree) so that the perfect reconstruction conditions are satisfied. Note that $h_i(n)$ and $g_i(n)$ have the same autocorrelation function

$$H_i(z)H_i(1/z) = G_i(z)G_i(1/z), \quad i = 0, 1, 2.$$

Therefore, if the PR conditions (5) are satisfied, then the PR conditions (7) are also satisfied. In addition, note that

$$G_i(z)G_i(-1/z) = A(z)A(-1/z)H_i(z)H_i(1/z)$$

for $i = 0, 1, 2$ and in turn

$$\sum_{i=0}^{2} G_i(z)G_i(-1/z) = A(z)A(-1/z) \times \sum_{i=0}^{2} H_i(z)H_i(-1/z).$$

Therefore, if the PR conditions (6) are satisfied, then the PR conditions (8) are also satisfied, so we only need to concentrate on (5) and (6).

Let us define the product filter $P_0(z)$ as

$$\begin{aligned} P_0(z) &:= H_0(z)H_0(1/z) = G_0(z)G_0(1/z) \\ &= D(z)D(1/z)(z + 2 + z^{-1})^{K_0}Q_0(z)Q_0(1/z) \\ &= D(z)D(1/z)(z + 2 + z^{-1})^{K_0}R_0(z) \end{aligned} \tag{32}$$

where

$$R_0(z) := Q_0(z)Q_0(1/z) \tag{33}$$

and for $i = 1, 2$, let us define the product filter $P_i(z)$ as

$$\begin{aligned} P_i(z) &:= H_i(z)H_i(1/z) = G_i(z)G_i(1/z) \\ &= D(-z)D(-1/z)(-z + 2 - z^{-1})^{K_i} \\ &\quad \times Q_i(z)Q_i(1/z). \end{aligned}$$

Then the perfect reconstruction conditions (5) and (7) can be written as

$$P_0(z) + P_1(z) + P_2(z) = 2. \tag{34}$$

In our examples, we will ask that the four wavelets have the same number of vanishing moments (then neither wavelet does more "work" than the other), that is, we will use $K_1 = K_2$ in the examples. Because this also simplifies the notation in the following derivation, in the remainder of the paper, we assume that $K_1 = K_2$. We also assume that $K_0 > K_1$. If we define

$$R_{12}(z) := Q_1(z)Q_1(1/z) + Q_2(z)Q_2(1/z)$$

then we can write

$$\begin{aligned} P_1(z) + P_2(z) &= D(-z)D(-1/z) \\ &\quad \times (-z + 2 - z^{-1})^{K_1}R_{12}(z). \end{aligned} \tag{35}$$

Combining (32) and (35), the PR conditions (5) and (7) are written as

$$\begin{aligned} 2 &= D(z)D(1/z)(z + 2 + z^{-1})^{K_0}R_0(z) \\ &\quad + D(-z)D(-1/z)(-z + 2 - z^{-1})^{K_1}R_{12}(z) \end{aligned} \tag{36}$$

where $r_0(n) = r_0(-n)$, and $r_{12}(n) = r_{12}(-n)$. Then, given K_0, K_1, and $D(z)$, we can find $R_0(z)$ and $R_{12}(z)$ straight forwardly by solving a linear system of equations or by using the extended Euclidean algorithm forgreatest common divisor (GCD) computations. From the Euclidean algorithm, we know in advance that $r_0(n)$ will be of length $2L + 2K_1 - 1$ and that $r_{12}(n)$ will be of length $2L + 2K_0 - 1$. The sequence $r_0(n)$ is supported on $1 - L - K_1 \le n \le L + K_1 - 1$, and $r_{12}(n)$ is supported on $1 - L - K_0 \le n \le L + K_0 - 1$. Once $R_0(z)$ is found, then $Q_0(z)$ can be obtained through spectral factorization from (33), which in turn gives $H_0(z)$ and $G_0(z)$. The length of $q_0(n)$ will be $L + K_1$. Note that $Q_0(z)$ is not unique, and neither is $H_0(z)$ nor $G_0(z)$. In the examples below, we take $Q_0(z)$ to be minimum-phase (all zeros of $Q_0(z)$ lie inside $|z| = 1$). The length of $h_0(n)$ and $g_0(n)$ will be $K_0 + K_1 + 2L$.

TABLE I
COEFFICIENTS OF (MINIMUM-PHASE) $q_0(n)$ WHEN $K_0 = 4, K_1 = K_2 = 2, L = 2$

n	$q_0(n)$
0	0.06911582051268
1	-0.05503365268588
2	0.01454236721253
3	-0.00100317639923

For example, when we have $K_0 = 4, K_1 = K_2 = 2, L = 2$, then the (minimum-phase) sequence $q_0(z)$ we obtain by this procedure is tabulated in Table I. The lowpass filters $h_0(n)$ and $g_0(n)$, both of length 10, are illustrated in Fig. 4, along with the frequency response and zero diagram of each. Note that $|H_0(e^{j\omega})| = |G_0(e^{j\omega})|$. The two zeros of $H_0(z)$ on the negative real axis are from $D(z)$, whereas the two zeros of $G_0(z)$ on the negative real axis are from and $D(1/z)$. The remaining zeros inside the unit circle are from $Q_0(z)$. Note that even though $Q_0(z)$ is minimum phase, $H_0(z)$ and $G_0(z)$ are not, due to the factors $D(z)$ and $D(1/z)$ in $H_0(z)$ and $G_0(z)$, respectively.

V. CONSTRUCTING THE WAVELET FILTERS

Once the lowpass filters $h_0(n)$ and $g_0(n)$ are obtained, the four (nonunique) wavelet filters $h_1(n), h_2(n), g_1(n)$, and $g_2(n)$ can be obtained using a polyphase formulation. We will concentrate on obtaining the filters $h_i(n)$, for then, the filters $g_i(n)$ follow from (21) and (22). Define the polyphase components $H_{i0}(z)$ and $H_{i1}(z)$ through

$$H_i(z) = H_{i0}(z^2) + z^{-1}H_{i1}(z^2), \quad i = 0, 1, 2 \tag{37}$$

and define the polyphase matrix $H(z)$ as

$$H(z) = \begin{bmatrix} H_{00}(z) & H_{10}(z) & H_{20}(z) \\ H_{01}(z) & H_{11}(z) & H_{21}(z) \end{bmatrix}.$$

Then, the three-channel filterbank of Fig. 1 can be redrawn as the filterbank of Fig. 5. Similarly, the perfect reconstruction condition can be written as

$$H(z)H^t(1/z) = I_2. \tag{38}$$

The matrix $H(z)$ is said to be a 2×3 *lossless* system [31]. Once we find four components H_{10}, H_{11}, H_{20}, and H_{21} so that $H(z)$ satisfies (38), we can then form $h_1(n)$ and $h_2(n)$.

One way to obtain a 2×3 lossless system is to first determine a 3×3 lossless system and to then delete the last row. Define $\hat{H}(z)$ to be the matrix

$$\hat{H}(z) = \begin{bmatrix} H_{00}(z) & H_{10}(z) & H_{20}(z) \\ H_{01}(z) & H_{11}(z) & H_{21}(z) \\ H_{02}(z) & H_{12}(z) & H_{22}(z) \end{bmatrix}$$

where only $H_{00}(z)$ and $H_{01}(z)$ are determined thus far. We will design the square lossless system $\hat{H}(z)$, or *paraunitary matrix*, to satisfy

$$\hat{H}^t(1/z)\hat{H}(z) = \hat{H}(z)\hat{H}^t(1/z) = I_3. \tag{39}$$

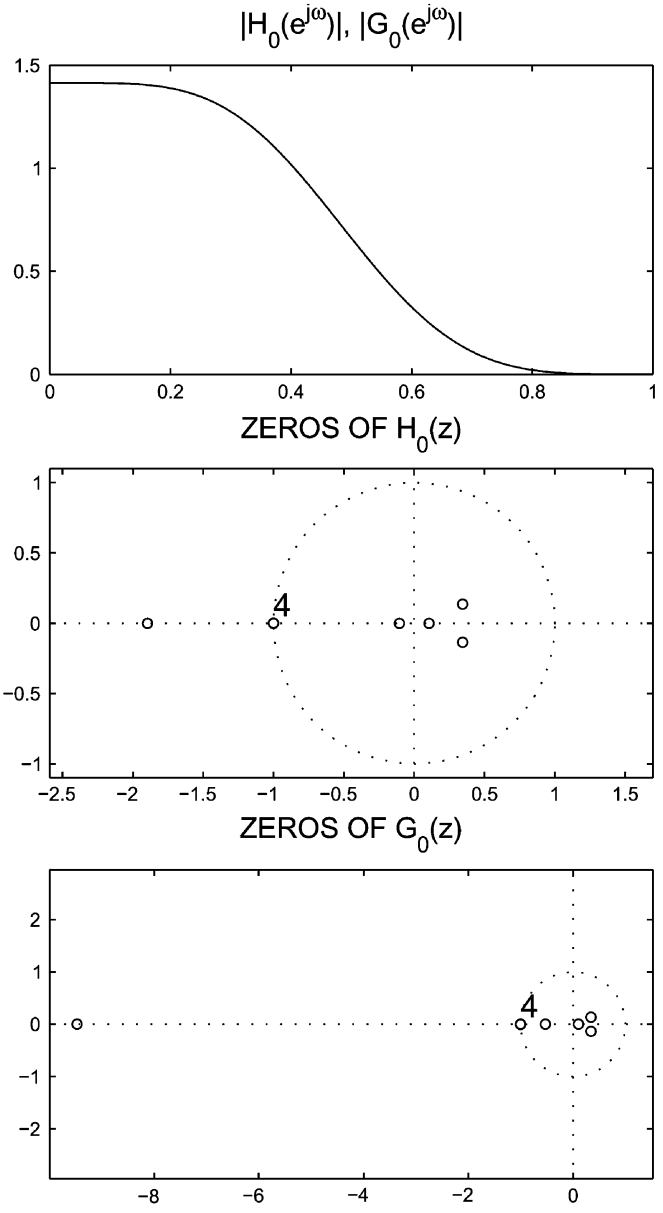

Fig. 4. Lowpass filters $h_0(n)$ and $g_0(n)$ obtained with $K_0 = 4, K_1 = K_2 = 2, L = 2$. The filter coefficients are tabulated in Table II.

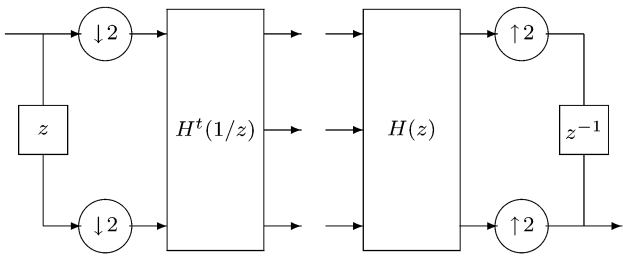

Fig. 5. Oversampled filterbank of Fig. 1 in polyphase form.

Then

$$H_{00}(z)H_{00}(1/z) + H_{01}(z)H_{01}(1/z) + H_{02}(z)H_{02}(1/z) = 1$$

or

$$H_{02}(z)H_{02}(1/z) = 1 - H_{00}(z)H_{00}(1/z) - H_{01}(z)H_{01}(1/z). \tag{40}$$

Therefore $H_{02}(z)$ can be obtained by spectral factorization

$$|H_{02}(e^{j\omega})|^2 = 1 - |H_{00}(e^{j\omega})|^2 - |H_{01}(e^{j\omega})|^2. \quad (41)$$

Note that $H_{02}(z)$ is not uniquely defined.

It turns out that the choice of $H_{02}(z)$ must be done here with care: Not just any spectral factor of the right-hand side of (41) will lead in what follows to filters $H_1(z), H_2(z)$ having the form set out in (18) and (19). It is shown in the appendix that the transfer function $H_{02}(z)$ in (41) must satisfy the following condition:

$$D(z)D(-z)|H_{02}(z^2)H_{i2}(1/z^2), \quad i = 0, 1, 2. \quad (42)$$

This suggests that $H_{02}(z)$ should satisfy the divisibility condition $D(z)D(-z)|H_{02}(z^2)$, which was verified numerically in examples to be the appropriate constraint on the spectral factorization of (41). Using the notation $[X(z)]_{\downarrow 2}$ to denote the Z-transform of $x(2n)$, we can write this condition as

$$[D(z)D(-z)]_{\downarrow 2}|H_{02}(z).$$

Similarly, it can be shown that $(1 - z^{-1})^{K_1}|H_{02}(z)$. Therefore

$$H_{02}(z) = [D(z)D(-z)]_{\downarrow 2}(1 - z^{-1})^{K_1}V(z)$$

where $V(z)$ is determined through spectral factorization according to (41).

Once we obtain $H_{02}(z)$, we have the first column of $\hat{H}(z)$. The remaining two columns of $\hat{H}(z)$ can be found using existing algorithms for paraunitary completion, for example, those described in [20], [31], or [32]. Once the 3×3 paraunitary matrix $\hat{H}(z)$ is completely known, the 2×3 matrix $H(z)$ is obtained by deleting the last row of $\hat{H}(z)$.

Define $E_0(z)$ to be the first column of $H(z)$ (now known)

$$E_0(z) := [H_{00}(z), H_{01}(z), H_{02}(z)]^t.$$

Then, $E_0(z)$ is a 3×1 lossless system, and as such, it can be factored as follows [31].

$$E_0(z) = U_N(z) \cdot U_{N-1}(z) \cdots U_1(z) \cdot P \quad (43)$$

with

$$U_k(z) = I_3 - u_k u_k^t + u_k u_k^t z^{-1}$$

where u_k and P are column vectors of unit norm. The minimal number of factors N is the McMillan degree of the system $E_0(z)$. The McMillan degree also gives the minimum number of delay elements required to implement a system.

Once the factorization (43) is determined, using the algorithm described in [31] and [32], a paraunitary matrix is obtained by replacing P with an orthogonal matrix $Q(Q^tQ = I_3)$, the first column of which is P. The resulting paraunitary matrix will have the same McMillan degree as $E_0(z)$.

Note that $U_k(1) = I_3$. Then, setting $z = 1$ in (43) gives

$$E_0(1) = U_N(1) \cdot U_{N-1}(1) \cdots U_1(1) \cdot P = P.$$

The column vector P is therefore uniquely determined by $H_{0i}(z)$. Note that $H_1(1) = H_2(1) = 0$, and hence, $P_1(1) = P_2(1) = 0$; therefore, from (34), we have $H_0(1) = \sqrt{2}$. In addition, note that $H_0(-1) = 0$. Therefore, from (37), we have

$$\begin{aligned} H_0(1) &= H_{00}(1) + H_{01}(1) \\ H_0(-1) &= H_{00}(1) - H_{01}(1) \end{aligned}$$

and in turn, it follows that $H_{00}(1) = H_{01}(1) = 1/\sqrt{2}$. From (40), we have $H_{02}(1) = 0$. Hence, the column vector P is given by

$$P = \frac{1}{\sqrt{2}}[1,\ 1,\ 0]^t. \quad (44)$$

Therefore, a 3×3 paraunitary matrix $\hat{H}(z)$, with $E_0(z)$ as the first column, is given by

$$\hat{H}(z) = U_N(z) \cdot U_{N-1}(z) \cdots U_1(z) \cdot Q$$

where Q is a 3×3 orthogonal matrix, the first column of which is P in (44). In this case, there is one degree of freedom in parameterizing Q. A simple parameterization of Q is given by

$$Q = \frac{1}{\sqrt{2}} \begin{bmatrix} 1 & 1 & 0 \\ 1 & -1 & 0 \\ 0 & 0 & \sqrt{2} \end{bmatrix} \quad \begin{bmatrix} 1 & 0 & 0 \\ 0 & \cos(\alpha_1) & -\sin(\alpha_1) \\ 0 & \sin(\alpha_1) & \cos(\alpha_1) \end{bmatrix}.$$

We will use the parameter α_1 to set the last coefficient of $h_2(n)$ to zero. It turns out that selecting α_1 in this way generally has the effect of making the last *two* coefficients of $h_2(n)$ equal to zero. (That is, $h_2(n)$ is two samples shorter than $h_0(n)$ and $h_1(n)$.) This effect was also observed in designing filters for the double-density DWT, as discussed in [24]. Becasue it is two samples shorter than $h_0(n)$ and $h_1(n)$, let us shift $h_2(n)$ by two samples. The PR conditions will still be satisfied. A new set of solutions can be obtained by then applying an orthogonal rotation operation to $h_1(n)$ and $h_2(n-2)$ as follows:

$$\begin{bmatrix} h_1(n) \\ h_2(n) \end{bmatrix} \leftarrow \begin{bmatrix} \cos(\alpha_2) & -\sin(\alpha_2) \\ \sin(\alpha_2) & \cos(\alpha_2) \end{bmatrix} \quad \begin{bmatrix} h_1(n) \\ h_2(n-2) \end{bmatrix}$$

where α_2 is selected to again set the last coefficient of the new $h_2(n)$ to zero. In our examples, we found that again, the last *two* coefficients of $h_2(n)$ turn out to be equal to zero. This procedure can be repeated until $h_2(n)$ is shorter than $h_0(n)$ and $h_1(n)$ by only one sample. Similar to what was observed in [24], this procedure has the effect of improving the shift relation between the two filters. Each time the shift and rotation is applied, the newly obtained filters $h_1(n)$ and $h_2(n)$ more nearly satisfy $h_1(n) = h_2(n-1)$, and the corresponding wavelets more nearly satisfy $\psi_{h,1}(t) = \psi_{h,2}(t - 0.5)$. In addition, it does not increase the support of $h_0(n)$ or $h_1(n)$ and increases the support of $h_2(n)$ by only one sample. Although this procedure may

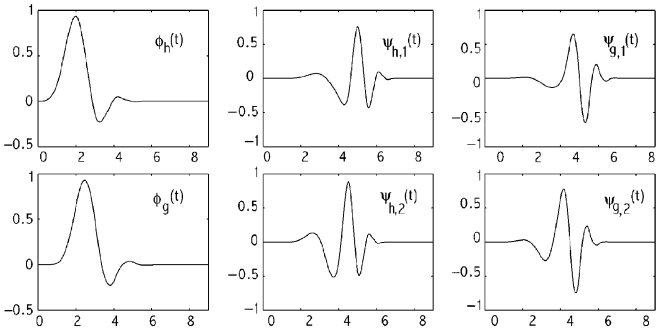

Fig. 6. Example 1. $K_0 = 4, K_1 = K_2 = 2, L = 2$. The filter coefficients are tabulated in Table II. The shift property and the envelopes of the complex wavelets are illustrated in Fig. 8.

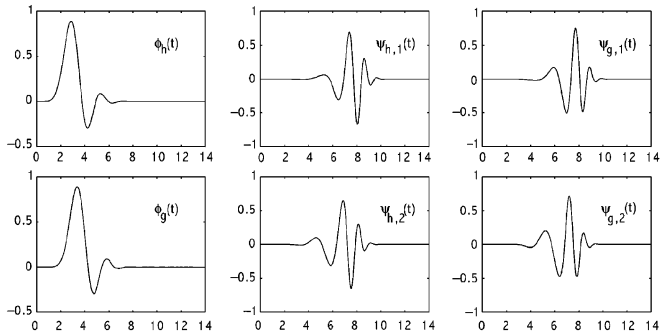

Fig. 7. Example 2. $K_0 = 6, K_1 = K_2 = 3, L = 3$. The filter coefficients are tabulated in Table III. The shift property and the envelopes of the complex wavelets are illustrated in Fig. 9.

not be optimal for obtaining wavelets satisfying (3), it is quite effective.

We note that we found the filterbank completion procedure outlined above to be prone to numerical problems when used for the examples given in the next section. This is likely due to the high-order zeros at $z = \pm 1$. However, by implementing the procedure in Maple and setting the arithmetic precision to 50 decimal digits, the examples were computed to very high accuracy, and this problem was entirely overcome. The filterbank completion algorithm of [20] may be more robust numerically, and therefore, it may offer another alternative.

VI. Examples

Figs. 6 and 7 illustrate two examples of sets of double-density dual-tree wavelets. Figs. 8 and 9 illustrate the shift properties and the envelopes of the complex wavelets.

1) Example 1: With $K_0 = 4, K_1 = K_2 = 2$, and $L = 2$, the filters obtained by following the design procedure described above are tabulated in Table II. The two scaling functions $\phi_h(t)$ and $\phi_g(t)$ and the four wavelet functions $\psi_{h,i}(t), \psi_{g,i}(t)$ are shown in Fig. 6. The integer translates of the four wavelets and their dyadic dilations form a (tight) frame. (A tight frame is one where the signal reconstruction can be performed with the transpose of the forward transform.) All of the wavelets have two vanishing moments. Note that $\psi_{h,1}(t) \approx \psi_{h,2}(t - 0.5)$ and $\psi_{g,1}(t) \approx \psi_{g,2}(t - 0.5)$, as illustrated in Fig. 8. That is, the filters $\{h_0, h_1, h_2\}$ form a double-density DWT, and similarly, $\{g_0, g_1, g_2\}$ also form one. In addition, we have $\psi_{g,1}(t) \approx \mathcal{H}\{\psi_{h,1}(t)\}$ and

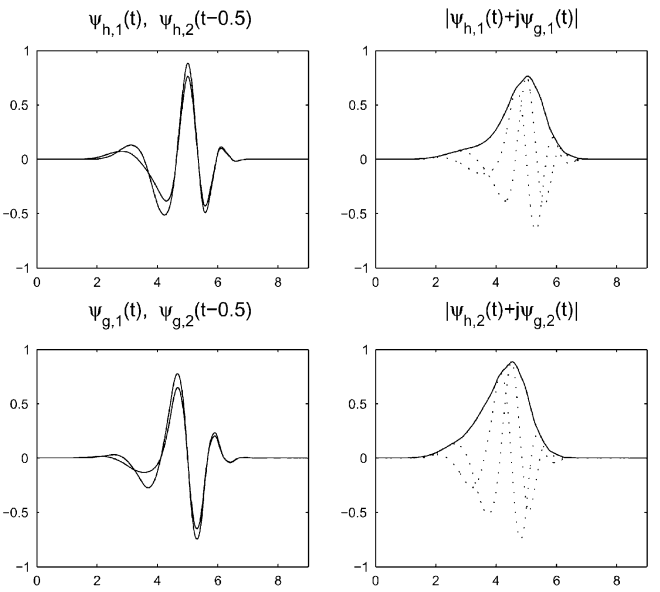

Fig. 8. Example 1. Shift property and the envelopes of the complex wavelets.

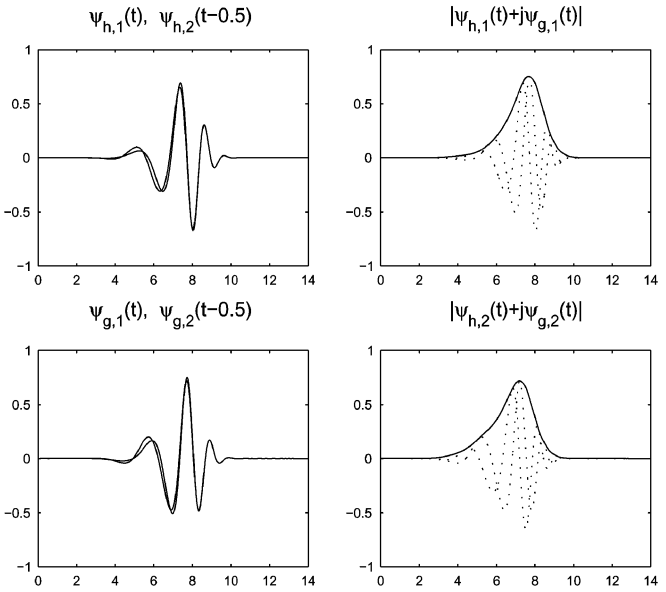

Fig. 9. Example 2. Shift property and the envelopes of the complex wavelets.

$\psi_{g,2}(t) \approx \mathcal{H}\{\psi_{h,2}(t)\}$; accordingly, the spectrum of the complex wavelet $\psi_{h,i}(t) + j\psi_{g,i}(t)$ is approximately single sided. A complex double-density DWT is formed by taking $\psi_{h,i}(t)$ and $\psi_{g,i}(t)$ to represent the real and imaginary parts of a single complex wavelet. Fig. 8 also illustrates the envelope function $\sqrt{\psi_{h,i}(t)^2 + \psi_{g,i}(t)^2} = |\psi_{h,i}(t) + j\psi_{g,i}(t)|$, which is the magnitude of the complex wavelet. Note that the envelope has a bell shape. To compare the double-density dual-tree transform with the dual-tree transform based on two critically sampled filter banks, Fig. 10 illustrates a pair of wavelets for the latter. They have the same support as those in Fig. 6 and are designed using the design procedure of [27], which also calls for a flat delay allpass filter. Using the same allpass filter (with $L = 2$), the wavelets can have a maximum of three vanishing moments. Note from the figure that the wavelets, as well as the envelope of the complex wavelet, do not have the same degree

TABLE II
COEFFICIENTS FOR EXAMPLE 1. $K_0 = 4, K_1 = K_2 = 2, L = 2$

n	$h_0(n)$	$h_1(n)$	$h_2(n)$
0	0.0691158205	0.0000734237	0.0001621689
1	0.3596612703	0.0003820788	0.0008438861
2	0.6657851023	-0.0059866448	-0.0136616968
3	0.4659189433	-0.0343385512	-0.0781278793
4	-0.0191014398	-0.0554428419	-0.0840435464
5	-0.1377522956	0.0018714327	0.2230705831
6	-0.0087922813	0.1386271745	0.3945086960
7	0.0194794983	0.3321168878	-0.6566499317
8	0.0000995795	-0.5661664438	0.2138977202
9	-0.0002006352	0.1888634841	0
n	$g_0(n)$	$g_1(n)$	$g_2(n)$
0	0.0138231641	0.0003671189	0.0008108446
1	0.1825175668	0.0048473455	0.0107061875
2	0.5537956151	0.0129572726	0.0264224754
3	0.6403205201	-0.0061082309	-0.0424847245
4	0.2024025378	-0.0656840149	-0.2095602589
5	-0.1327035751	-0.0968519623	-0.0055184660
6	-0.0714378446	-0.0211208454	0.6504107366
7	0.0179754457	0.5492354832	-0.4735663386
8	0.0085233088	-0.4154148634	0.0427795440
9	-0.0010031763	0.0377726968	0

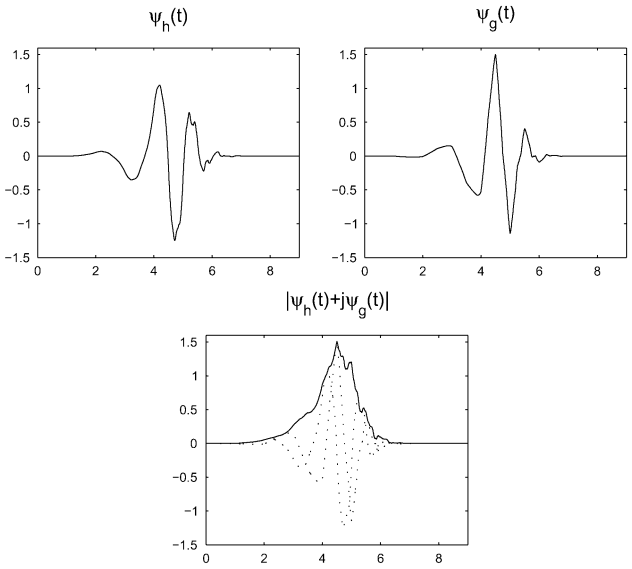

Fig. 10. Pair of wavelets corresponding to the dual-tree wavelet transform.

of smoothness as what can be achieved with the double-density dual-tree.

2) Example 2: When we take $K_0 = 6, K_1 = K_2 = 3$, and $L = 3$, we obtain the filters tabulated in Table III. The wavelets are illustrated in Figs. 7 and 9. In this example, the wavelets have three vanishing moments. Compared with the previous example, they more nearly satisfy $\psi_{g,i}(t) = \mathcal{H}\{\psi_{h,i}(t)\}, \psi_{h,1}(t) = \psi_{h,2}(t - 0.5)$, and $\psi_{g,1}(t) = \psi_{g,2}(t - 0.5)$, as illustrated in Fig. 9.

VII. CONCLUSION

This paper has introduced the double-density dual-tree DWT: a discrete wavelet transform that has properties of both

TABLE III
COEFFICIENTS FOR EXAMPLE 2. $K_0 = 6, K_1 = K_2 = 3, L = 3$

n	$h_0(n)$	$h_1(n)$	$h_2(n)$
0	0.0116751500	0.0000002803	0.0000009631
1	0.1121045343	0.0000026917	0.0000092482
2	0.3902035988	-0.0000945824	-0.0003285657
3	0.6376600221	-0.0009828317	-0.0034113692
4	0.4515927116	-0.0032260080	-0.0098485834
5	-0.0177905271	-0.0033984723	0.0011435281
6	-0.1899509889	0.0053478454	0.0535846285
7	-0.0363317137	0.0269410607	0.0710003404
8	0.0511638041	0.0499929334	-0.0732656061
9	0.0130979774	-0.0076424664	-0.2335672955
10	-0.0081410874	-0.2115533011	-0.0478802585
11	-0.0016378610	-0.1367235355	0.5808457358
12	0.0005650673	0.6180972127	-0.4014544851
13	0.0000043492	-0.3981725189	0.0631717194
14	-0.0000014745	0.0614116921	0
n	$g_0(n)$	$g_1(n)$	$g_2(n)$
0	0.0016678785	0.0000019623	0.0000067421
1	0.0427009907	0.0000502404	0.0001726122
2	0.2319241351	0.0002359631	0.0007854598
3	0.5459409911	-0.0003026422	-0.0016861130
4	0.6090383368	-0.0044343824	-0.0181424716
5	0.2145936637	-0.0123017187	-0.0350847982
6	-0.1629587558	-0.0156330903	0.0180629832
7	-0.1283958243	0.0044955076	0.1356963431
8	0.0309676536	0.0781684245	0.0980877181
9	0.0373820215	0.1319270081	-0.1963413775
10	-0.0038525812	-0.1244353736	-0.3762491967
11	-0.0053106600	-0.4465930970	0.5674107094
12	0.0003304362	0.5772994700	-0.2017431422
13	0.0001955983	-0.1972513705	0.0090245313
14	-0.0000103221	0.0087730988	0

the double-density DWT [24] and the dual-tree DWT [13]. The filterbank structure corresponding to this DWT consists of a pair of iterated oversampled filterbanks operating in parallel. Each iterated filterbank is of the form described in [24] and is redundant by a factor of 2. The total redundancy is therefore a factor of 4. The four wavelets are designed so that they form two approximate Hilbert transform pairs and so that the integer translates of one pair fall midway between the integer translates of the other pair. The paper has also developed a design procedure to obtain FIR filters that satisfy the numerous constraints imposed. This design procedure, which draws from the methods described in [3], [23], [24], and [27], employs a fractional-delay allpass filter, spectral factorization, and filterbank completion.

Further questions related to the double-density dual-tree wavelet transform are the design of wavelets with symmetries, which is important in many image processing applications. Instead of using tight wavelet frames (as here), to obtain symmetric wavelets having the sought properties, it will be useful to employ dual wavelet frames and techniques for their design [6], [10]. Because the application of the dual-tree DWT to image processing is of particular interest (due to the directional selectivity of the wavelets), the use of the double-density dual-tree DWT with symmetric wavelets for applications including image denoising and restoration is currently under investigation.

APPENDIX
CONDITION ON $H_{02}(z)$

By expanding in terms of polyphase components, it can be shown that

$$H_0(z)H_0(1/z) + H_0(-z)H_0(-1/z) = 2[H_{00}(z^2)H_{00}(1/z^2) + H_{01}(z^2)H_{01}(1/z^2)].$$

Therefore, (40) can be rewritten as

$$\begin{aligned} &H_{02}(z^2)H_{02}(1/z^2) \\ &\quad = 1 - 0.5[H_0(z)H_0(1/z) + H_0(-z)H_0(-1/z)] \\ &\quad = 1 - 0.5P_0(z) - 0.5P_0(-z). \end{aligned}$$

As $P_0(z) + P_1(z) + P_2(z) = 2$ from (34), we can write $1 - 0.5P_0(-z) = 0.5P_1(-z) + 0.5P_2(-z)$

$$H_{02}(z^2)H_{02}(1/z^2) = -0.5P_0(z) + 0.5P_1(-z) + 0.5P_2(-z).$$

From (32) and (35), we can write this as

$$\begin{aligned} &H_{02}(z^2)H_{02}(1/z^2) = 0.5D(z)D(1/z)(z + 2 + z^{-1})^{K_1} \cdot \\ &[R_z(z + 2 + z^{-1})^{K_0 - K_1} - R_{12}(-z)] \end{aligned}$$

that is

$$D(z)D(1/z)(z + 2 + z^{-1})^{K_1} \mid H_{02}(z^2)H_{02}(1/z^2).$$

As $H_{02}(z^2)H_{02}(1/z^2)$ is an even function of z, we deduce that

$$D(z)D(1/z)D(-z)D(-1/z)(z^2 + 2 + z^{-2})^{K_1}$$

divides into $H_{02}(z^2)H_{02}(1/z^2)$.

To derive (42) with $i = 1$, note from (39) that

$$H_{00}(z)H_{10}(1/z) + H_{01}(z)H_{11}(1/z) + H_{02}(z)H_{12}(1/z) = 0.$$

In addition, note (by expanding in terms of polyphase components) that

$$H_0(z)H_1(1/z) + H_0(-z)H_1(-1/z) = 2[H_{00}(z^2)H_{10}(1/z^2) + H_{01}(z^2)H_{11}(1/z^2)].$$

Therefore, $H_{02}(z^2)H_{12}(1/z^2)$ is given by

$$-0.5[H_0(z)H_1(1/z) + H_0(-z)H_1(-1/z)].$$

From (18) and (19), we then have that

$$D(z)D(-z) \mid H_{02}(z^2)H_{12}(1/z^2).$$

Condition (42), with $i = 2$, is derived similarly.

REFERENCES

[1] P. Abry, *Ondelettes et Turbulences*. Paris, France: Diderot, 1997.

[2] P. Abry and P. Flandrin, "Multiresolution transient detection," in *Proc. IEEE-SP Int. Symp. Time-Frequency Time-Scale Anal.*, Philadelphia, PA, Oct. 1994, pp. 225–228.

[3] C. Chui and W. He, "Compactly supported tight frames associated with refinable functions," *Appl. Comput. Harmon. Anal.*, vol. 8, no. 3, pp. 293–319, May 2000.

[4] C. K. Chui, W. He, and J. Stöckler, "Compactly supported tight and sibling frames with maximum vanishing moments," *Appl. Comput. Harmon. Anal.*, vol. 13, no. 3, pp. 177–283, Nov. 2003.

[5] R. R. Coifman and D. L. Donoho, "Translation-invariant de-noising," in *Wavelets and Statistics*, A. Antoniadis, Ed. New York: Springer-Verlag, 1995.

[6] I. Daubechies and B. Han, "Pairs of dual wavelet frames from any two refinable functions," Constr. Approx, to be published.

[7] I. Daubechies, B. Han, A. Ron, and Z. Shen, "Framelets: MRA-based constructions of wavelet frames," *Appl. Comput. Harmon. Anal.*, vol. 14, no. 1, pp. 1–46, 2003.

[8] F. Fernandes, R. van Spaendonck, and C. S. Burrus, "A new directional, low-redundancy complex-wavelet transform," in *Proc. IEEE Int. Conf. Acoust., Speech, Signal Process.*, May 2001.

[9] W. T. Freeman and E. H. Adelson, "The design and use of steerable filters," *IEEE Trans. Pattern Anal. Machine Intell.*, vol. 13, pp. 891–906, Sept. 1991.

[10] B. Han, "On dual wavelet tight frames," *Appl. Comput. Harmon. Anal.*, vol. 4, pp. 380–413, 1997.

[11] N. G. Kingsbury, "The dual-tree complex wavelet transform: A new technique for shift invariance and directional filters," in *Proc. Eighth IEEE DSP Workshop*, Salt Lake City, UT, Aug. 9–12, 1998.

[12] ——, "Image processing with complex wavelets," *Phil. Trans. R. Soc. London A*, Sept. 1999.

[13] ——, "Complex wavelets for shift invariant analysis and filtering of signals," *Appl. Comput. Harmon. Anal.*, vol. 10, no. 3, pp. 234–253, May 2001.

[14] T. I. Laakso, V. Välimäki, M. Karjalainen, and U. K. Laine, "Splitting the unit delay," *IEEE Signal Processing Mag.*, vol. 13, pp. 30–60, Jan. 1996.

[15] M. Lang, H. Guo, J. E. Odegard, C. S. Burrus, and R. O. Wells Jr., "Noise reduction using an undecimated discrete wavelet transform," *IEEE Signal Processing Lett.*, vol. 3, pp. 10–12, Jan. 1996.

[16] J. Liu and P. Moulin, "Translation invariant wavelet denoising of Poisson data," in *Proc. Conf. Inform. Sci. Syst.*. Baltimore, MD, Mar. 21–23, 2001, pp. 878–883.

[17] G. P. Nason and B. W. Silverman, "Stationary wavelet transform and some statistical applications," in *Wavelets and Statistics*, A. Antoniadis, Ed. New York: Springer-Verlag, 1995, pp. 281–299.

[18] A. Petukhov, "Symmetric framelets," *Constr. Approx.*, vol. 19, no. 2, pp. 309–328, Jan. 2003.

[19] ——, "Explicit construction of framelets," *Appl. Comput. Harmon. Anal.*, vol. 11, no. 2, pp. 313–327, Sept. 2001.

[20] C. Popeea, B. Dumitrescu, and B. Jora, "An efficient algorithm for filter bank completion," in *Proc. IEEE Int. Conf. Acoust., Speech, Signal Process.*, May 2001.

[21] A. Ron and Z. Shen, "Affine systems in $L_2(\mathbb{R}^d)$: The analysis of the analysis operator," *J. Funct. Anal.*, vol. 148, pp. 408–447, 1997.

[22] ——, "Construction of compactly supported affine frames in $L_2(\mathbb{R}^d)$," in *Advances in Wavelets*, K. S. Lau, Ed. New York: Springer-Verlag, 1998.

[23] I. W. Selesnick, "The design of Hilbert transform pairs of wavelet bases via the flat delay filter," in *Proc. IEEE Int. Conf. Acoust., Speech, Signal Process.*, May 2001.

[24] ——, "The double density DWT," in *Wavelets in Signal and Image Analysis: From Theory to Practice*, A. Petrosian and F. G. Meyer, Eds. Boston, MA: Kluwer, 2001.

[25] ——, "Hilbert transform pairs of wavelet bases," *IEEE Signal Processing Lett.*, vol. 8, pp. 170–173, June 2001.

[26] ——, "Smooth wavelet tight frames with zero moments," *Appl. Comput. Harmon. Anal.*, vol. 10, no. 2, pp. 163–181, Mar. 2001.

[27] ——, "The design of approximate Hilbert transform pairs of wavelet bases," *IEEE Trans. Signal Processing*, vol. 50, pp. 1144–1152, May 2002.

[28] E. P. Simoncelli and W. T. Freeman, "The steerable pyramid: A flexible architecture for multi-scale derivative computation," in *Proc. IEEE Int. Conf. Image Process.*, Washington, DC, Oct. 1995.

[29] E. P. Simoncelli, W. T. Freeman, E. H. Adelson, and D. J. Heeger, "Shiftable multi-scale transforms," *IEEE Trans. Inform. Theory*, vol. 38, pp. 587–607, Mar. 1992.

[30] J. P. Thiran, "Recursive digital filters with maximally flat group delay," *IEEE Trans. Circuit Theory*, vol. CT-18, pp. 659–664, Nov. 1971.

[31] P. P. Vaidyanathan, *Multirate Systems and Filter Banks*. Englewood Cliffs, NJ: Prentice-Hall, 1993.

[32] P. P. Vaidyanathan, T. Q. Nguyen, Z. Doğanata, and T. Saramäki, "Improved technique for design of perfect reconstruction FIR QMF banks with lossless polyphase matrices," in *IEEE Trans. Acoust., Speech, Signal Process.*, vol. 37, July 1989, pp. 1042–1056.

Ivan Selesnick (M'95) received the B.S., M.E.E., and Ph.D. degrees in electrical engineering in 1990, 1991, and 1996, respectively, from Rice University, Houston, TX.

In 1997, he was a visiting professor at the University of Erlangen-Nürnberg, Nürnberg, Germany. Since 1997, he has been with the Department of Electrical and Computer Engineering, Polytechnic University, Brooklyn, NY, where he is currently an Associate Professor. His current research interests are in the area of digital signal processing and wavelet-based signal processing.

Dr. Selesnick is currently a member of the IEEE Signal Processing Theory and Methods Technical Committee and an associate editor of the IEEE TRANSACTIONS ON IMAGE PROCESSING. In 2003, he received a Jacobs Excellence in Education Award.